Derivatives of the local ballooning growth rate with respect to surface label, field line label, and ballooning parameter

S. R. Hudson

Princeton Plasma Physics Laboratory, P.O. Box 451, Princeton, New Jersey 08543

Expressions for the derivative of the local ballooning growth rate with respect to surface label, field line label, and ballooning-parameter are presented. Such expressions lead to increased computational efficiency for ballooning stability applications. © *2006 American Institute of Physics*. [DOI: 10.1063/1.2193537]

I. INTRODUCTION

For comprehensive ballooning analysis in three-dimensional (stellarator) systems, an extensive set of ballooning eigenvalue calculations is generally required. For several applications, it is convenient to know how the local ballooning stability will change as a function of the surface label, ψ, the field line label, α, and the angle-like ballooning parameter, θ_k. For instance, it is typically the most unstable field line that sets the stability limit. The derivatives of the growth rate with respect to (ψ, α, θ_k) allow efficient algorithms to be applied to search for the most unstable field line, or to trace out marginal stability boundaries.

A particularly important application is in the ray tracing problem,[1] when results from the local ballooning analysis are extended to make predictions regarding the global stability.

The standard approach to performing the ray tracing is to first compute the eigenvalue on a (ψ, α, θ_k) lattice,[2,3] and to then take the derivatives numerically. This approach has certain disadvantages. Typically, accuracy is lost when derivatives are taken numerically; the eigenvalue lattice must be constructed at sufficiently high resolution to ensure that the interpolation is accurate. Also, this approach does not easily allow the accuracy of the calculation to be easily improved; if the ballooning eigenvalue calculation itself is to be refined, the eigenvalue lattice must be reconstructed.

This article presents an explicit method for calculating the derivatives. The method is an application of eigenvalue perturbation analysis. For a small variation in (ψ, α, θ_k), the induced small variation in the ballooning operator may be determined by differentiating the ballooning coefficients. Using operator perturbation theory, the induced variation in the eigenvalue, and thus the eigenvalue derivatives, can then be determined.

A similar analysis was applied to determine the impact of variations in both the pressure gradient and shear on ballooning stability to predict which configurations would display the second stability.[4,5]

In Sec. II, a convenient form for the ballooning equation is given. In Sec. III, it is shown how variations in the coordinates (ψ, α, θ_k) affect the coefficients of the ballooning equation. Operator perturbation theory is then used to determine the required derivatives. Section IV illustrates how the derivative information can be used to increase the accuracy of eigenvalue lattice interpolation.

II. BALLOONING EQUATION

Using straight field line coordinates (θ, ζ), the magnetic field takes the form

$$\mathbf{B} = q \, \nabla \, \psi \times \nabla \theta + \nabla \zeta \times \nabla \psi, \tag{1}$$

where $2\pi\psi$ is the poloidal magnetic flux and $q(\psi)$ is the inverse rotational transform (safety factor). This article shall use the (θ, ζ) of Boozer coordinates,[6] which allows the covariant representation

$$\mathbf{B} = \beta(\psi, \theta, \zeta) \, \nabla \, \psi + I(\psi) \, \nabla \, \theta + G(\psi) \, \nabla \, \zeta. \tag{2}$$

Changing the toroidal coordinate from ζ to $\alpha = \zeta - q\theta$, the magnetic field then becomes

$$\mathbf{B} = \nabla \alpha \times \nabla \psi. \tag{3}$$

The $\mathbf{B} \cdot \nabla$ operator becomes

$$\mathbf{B} \cdot \nabla = \sqrt{g}^{-1} \left. \frac{\partial}{\partial \theta} \right|_{\psi, \alpha} \tag{4}$$

where the notation $\partial f / \partial x|_{y,z}$ indicates the partial derivative of f with respect to x, with y and z held constant.

Stability is determined by calculating the growth rate of a small displacement from an equilibrium. To treat ballooning modes,[1] the plasma displacement is written

$$\boldsymbol{\xi}(\mathbf{x}) = \hat{\boldsymbol{\xi}}(\mathbf{x}) \exp(iS(\mathbf{x})/\epsilon - i\omega t) \tag{5}$$

with the wave vector $\mathbf{k} \equiv \nabla S$. The ballooning ordering requires $\mathbf{k} \cdot \mathbf{B} = 0$. This, with the form of the magnetic field Eq. (3), requires the eikonal function to be of the form $S = S(\psi, \alpha)$. The wave vector is then

$$\mathbf{k} = k_\alpha \, \nabla \, \alpha + k_\psi \, \nabla \, \psi \equiv k_\alpha (\nabla \alpha + q' \theta_k \, \nabla \, \psi), \tag{6}$$

where the ballooning parameter $\theta_k = k_\psi / q' k_\alpha$. The definition of θ_k is consistent with that used by Dewar and Glasser,[1] but here ψ is retained as the surface label, whereas Dewar and Glasser use q as the surface label. For incompressible perturbations, $\nabla \cdot \boldsymbol{\xi} = 0$, and to lowest order in ϵ, the perturbation may be written

$$\hat{\xi}^{(0)} = \xi \frac{\mathbf{B} \times \mathbf{k}}{B^2 k_\alpha} + \eta \mathbf{B}. \tag{7}$$

The ballooning equation is[3]

$$\mathbf{B} \cdot \nabla \frac{k^2}{B^2 k_\alpha^2} \mathbf{B} \cdot \nabla \xi + 2 \frac{\mathbf{B} \times \mathbf{k} \cdot \kappa}{B^2 k_\alpha} \frac{\mathbf{B} \times \mathbf{k} \cdot \nabla p}{B^2 k_\alpha} \xi$$

$$= - \omega^2 \rho \frac{k^2}{B^2 k_\alpha^2} \xi, \tag{8}$$

where $B^2 \kappa = \nabla_\perp (B^2/2 + \mu_0 p)$ is the curvature, which may be written

$$\kappa = \kappa_n \nabla \psi + \kappa_g \mathbf{B} \times \nabla \psi / g^{\psi\psi}. \tag{9}$$

Ballooning stability is determined by a competition between the destabilizing influences of pressure gradients in regions of unfavorable curvature, and the stabilizing influence of field line bending due to the local shear. Defining the local shear s by

$$s = \sqrt{g} \frac{-\mathbf{B} \times \nabla \psi}{g^{\psi\psi}} \cdot \nabla \times \frac{\mathbf{B} \times \nabla \psi}{g^{\psi\psi}}, \tag{10}$$

and the quantity L by

$$L = \frac{g^{\psi\alpha}}{g^{\psi\psi}} + q' \theta_k, \tag{11}$$

it is observed that

$$s = \sqrt{g} \mathbf{B} \cdot \nabla L. \tag{12}$$

The quantity L is called the (field line) integrated local shear, and the ballooning parameter θ_k appears to play the role of an integration constant. The integrated local shear may also be written, using the (θ, ζ) of Boozer coordinates,

$$L = - q'(\theta - \theta_k) + L_s, \tag{13}$$

where $-q'(\theta - \theta_k)$ is a secular term that increases along the field line, and $L_s = (G g_{\psi\theta} - I g_{\psi\zeta})/\sqrt{g} g^{\psi\psi}$ is a function of position (ψ, θ, ζ).

The ballooning equation may now be written

$$\left[\left. \frac{\partial}{\partial \theta} \right|_{\psi,\alpha} P \left. \frac{\partial}{\partial \theta} \right|_{\psi,\alpha} + Q - \lambda R \right] \xi = 0, \tag{14}$$

where the ballooning coefficients are

$$P(\psi, \alpha, \theta; \theta_k) = B^2 / g^{\psi\psi} + g^{\psi\psi} L, \tag{15}$$

$$Q(\psi, \alpha, \theta; \theta_k) = 2p' \sqrt{g} (I + qG)(\kappa_n + \kappa_g L), \tag{16}$$

$$R(\psi, \alpha, \theta; \theta_k) = \rho \sqrt{g}^2 P, \tag{17}$$

and the eigenvalue $\lambda = -\omega^2$. This form for the ballooning equation was used by Hegna and Nakajima,[7] and is a convenient form for constructing marginal stability diagrams.[8,4]

For general three-dimensional configurations, the local ballooning growth rate is a function of the field line, labeled by ψ and α, and the ballooning parameter θ_k:

$$- \omega^2 = \lambda(\psi, \alpha, \theta_k), \tag{18}$$

and the required first order derivatives satisfy

$$\delta \lambda = \left. \frac{\partial \lambda}{\partial \psi} \right|_{\alpha, \theta_k} \delta \psi + \left. \frac{\partial \lambda}{\partial \alpha} \right|_{\psi, \theta_k} \delta \alpha + \left. \frac{\partial \lambda}{\partial \theta_k} \right|_{\psi, \alpha} \delta \theta_k, \tag{19}$$

for infinitesimal variations $\delta\psi$, $\delta\alpha$, and $\delta\theta_k$.

Before proceeding to the operator perturbation theory, it is convenient to first describe the numerical solution to solving Eq. (14). The ballooning equation is efficiently solved using a finite difference method on a field line grid. The field line grid $\{(\theta_i, \zeta_i) : i = -N, N\}$ is given by

$$\theta_i = i \theta_\infty / N + \theta_k, \tag{20}$$

$$\zeta_i = \alpha + q \theta_i, \tag{21}$$

where θ_∞ is chosen sufficiently large to contain the mode, and N determines the resolution of the field line grid. Note that the field line grid for θ_i is centered on θ_k. The equation to be solved becomes a set of $2N - 1$ linear equations of the form

$$\frac{P_{i+\frac{1}{2}}}{\Delta} \frac{(\xi_{i+1} - \xi_i)}{\Delta} - \frac{P_{i-\frac{1}{2}}}{\Delta} \frac{(\xi_i - \xi_{i-1})}{\Delta} + Q_i \xi_i = \lambda R_i \xi_i, \tag{22}$$

where $\Delta = \theta_\infty / N$. Here, Q_i and R_i are calculated on the full grid, whereas $P_{i+1/2}$ is calculated on the half-grid. This is a matrix equation, $M\xi = \lambda\xi$, where M is tridiagonal. The largest eigenvalue and its eigenfunction are then solved using standard numerical routines.[9,10] For the following, it is assumed that the corresponding eigenvector has also been calculated. Note that as the ballooning coordinates (ψ, α, θ_k) are changed, the field line grid will change.

It is worth noting that this construction guarantees that the poloidal and toroidal symmetries[1]

$$\lambda(\psi, \alpha + 2\pi, \theta_k) = \lambda(\psi, \alpha - 2\pi q, \theta_k + 2\pi) = \lambda(\psi, \alpha, \theta_k) \tag{23}$$

hold, for any finite θ_∞. If the field line grid for θ_i was not centered about θ_k, the eigenvalue symmetry $\lambda(\psi, \alpha - 2\pi q, \theta_k + 2\pi) = \lambda(\psi, \alpha, \theta_k)$ may not be preserved numerically for finite θ_∞.

III. VARIATIONS

It is important to distinguish the different coordinate systems employed. A point in physical space is given by the three coordinates (ψ, θ, ζ), whereas the ballooning eigenvalue, λ, is a function of (ψ, α, θ_k).

On a variation of the ballooning coordinates (ψ, α, θ_k), the physical space coordinates vary, and the ballooning coefficients vary. Because the field line grid depends on the field line, labelled by ψ, α, and that the field line grid is adjusted to remain centered about θ_k, the physical space coordinates of the field line grid vary according to

$$\delta \psi_i = \delta \psi, \tag{24}$$

$$\delta \theta_i = \delta \theta_k, \tag{25}$$

$$\delta \zeta_i = \delta \alpha + q' \theta_i \delta \psi + q \delta \theta_k. \tag{26}$$

The variation of the ballooning coefficient, δP, is given by

$$\delta P = \frac{2B\delta B}{g^{\psi\psi}} - \frac{B^2}{g^{\psi\psi}}\frac{\delta g^{\psi\psi}}{g^{\psi\psi}} + \delta g^{\psi\psi}L^2 + g^{\psi\psi}2L\delta L. \quad (27)$$

The expressions for δQ and δR take similar forms.

The terms δB and $\delta g^{\psi\psi}$, and terms such as $\delta\kappa_n, \delta\kappa_g$ which appear in the expression for δQ, take the form

$$\delta f = \left.\frac{\partial f}{\partial\psi}\right|_{\theta,\zeta}\delta\psi + \left.\frac{\partial f}{\partial\theta}\right|_{\psi,\zeta}\delta\theta + \left.\frac{\partial f}{\partial\zeta}\right|_{\psi,\theta}\delta\zeta, \quad (28)$$

where f is an arbitrary function of position $f = f(\psi,\theta,\zeta)$. Combining this expression with Eqs. (24)–(26), an expression for all quantities which are functions of physical space is given by

$$\delta f = \left(\left.\frac{\partial f}{\partial\psi}\right|_{\theta,\zeta} + q'\theta\left.\frac{\partial f}{\partial\zeta}\right|_{\psi,\theta}\right)\delta\psi + \left.\frac{\partial f}{\partial\zeta}\right|_{\psi,\theta}\delta\alpha$$
$$+ \left(\left.\frac{\partial f}{\partial\theta}\right|_{\psi,\zeta} + q\left.\frac{\partial f}{\partial\zeta}\right|_{\psi,\theta}\right)\delta\theta_k. \quad (29)$$

The term δL is slightly different due to the secular term:

$$\delta L = -q''(\theta - \theta_k)\delta\psi + \delta L_s, \quad (30)$$

where δL_s is of the form given in Eq. (29).

The above expressions may be combined and δP is written

$$\delta P = \partial_\psi P|_{\alpha,\theta_k}\delta\psi + \partial_\alpha P|_{\psi,\theta_k}\delta\alpha + \partial_{\theta_k}P|_{\psi,\alpha}\delta\theta_k, \quad (31)$$

similarly for δQ and δR. The full expressions for $\partial_\psi P|_{\alpha,\theta_k}$, etc. are quite lengthy. The expression for δQ involves the spatial derivatives of the normal and geodesic curvatures, κ_n and κ_g. Using the (θ,ζ) of Boozer coordinates, the curvatures are written

$$\kappa_n = \frac{1}{B^2}\frac{\partial}{\partial\psi}\left(\frac{B^2}{2} + \mu_0 p\right) + \frac{\beta(q\partial_\zeta\sqrt{g} + \partial_\theta\sqrt{g})}{2\sqrt{g}(I + qG)}$$
$$+ \frac{(Gg_{\psi\theta} - Ig_{\psi\zeta})}{\sqrt{g}g^{\psi\psi}}\frac{(G\partial_\theta\sqrt{g} - I\partial_\zeta\sqrt{g})}{2\sqrt{g}(I + qG)}, \quad (32)$$

$$\kappa_g = \frac{I\partial_\zeta\sqrt{g} - G\partial_\theta\sqrt{g}}{2\sqrt{g}(I + qG)}, \quad (33)$$

where the derivatives are given by $\partial_\theta \equiv \partial/\partial\theta|_{\psi,\zeta}$, $\partial_\zeta \equiv \partial/\partial\zeta|_{\psi,\theta}$. The radial derivative of the normal curvature will involve the second radial derivative of the magnetic field strength, B. The second radial derivatives of the q profile, pressure, and various metric quantities will also be required in the ultimate calculation of the eigenvalue derivatives.

Upon variation, the ballooning equation is written

$$\left[\left.\frac{\partial}{\partial\theta}\right|_{\psi,\alpha}(P + \delta P)\left.\frac{\partial}{\partial\theta}\right|_{\psi,\alpha} + (Q + \delta Q)\right](\xi + \delta\xi)$$
$$= (\lambda + \delta\lambda)(R + \delta R)(\xi + \delta\xi). \quad (34)$$

Using the Hermitian property of the operators, the derivatives of the eigenvalue are then given by expressions of the form

$$\left.\frac{\partial\lambda}{\partial\psi}\right|_{\alpha,\theta_k} = \left\langle\xi\left|\left.\frac{\partial}{\partial\theta}\right|_{\psi,\alpha}\partial_\psi P|_{\alpha,\theta_k}\left.\frac{\partial}{\partial\theta}\right|_{\psi,\alpha}\right.\right.$$
$$\left.\left. + \partial_\psi Q|_{\alpha,\theta_k} - \lambda\partial_\psi R|_{\alpha,\theta_k}\right|\xi\right\rangle,$$

where the bracket notation indicates the normalized inner product $\langle\xi|f|\xi\rangle = \int\xi f\xi d\theta / \int\xi R\xi d\theta$.

IV. APPLICATION

To illustrate the benefits of direct calculation of the derivatives over the alternatives, an equilibrium relevant to the LHD stellarator has been examined. The equilibrium itself is calculated using the VMEC code, and the equilibrium is then mapped to Boozer coordinates. The determination of the derivatives described above has been implemented numerically.

This section will make some comparisons between the construction of the ballooning eigenvalue derivatives presented in this article to the determination of the derivatives provided by a standard ballooning code—that is in this context, a ballooning code that only calculates the ballooning eigenvalue.

Consider the determination of the eigenvalues at an arbitrary point in ballooning space (ψ, α, θ_k). The direct method requires only one evaluation: the eigenvalue and the derivatives are returned simultaneously. Also, the accuracy of the derivatives is consistent with the accuracy of the eigenvalue, both being determined by the resolution of the field line grid as described in Eqs. (20) and (21). Note that to determine the derivatives, additional Fourier summations are required to determine the variation in the ballooning coefficients. This is an additional computational burden, but a modest one and the computational cost of determining the eigenvalue and its derivatives is only slightly greater than determining the eigenvalue alone.

Using a ballooning code that only returns the eigenvalue, the derivatives may be determined

$$\left.\frac{\partial\lambda}{\partial\psi}\right|_{\alpha,\theta_k} = \frac{\lambda(\psi + h, \alpha, \theta_k) - \lambda(\psi, \alpha, \theta_k)}{h} + O(h), \quad (35)$$

and similarly for $\partial\lambda/\partial\alpha$ and $\partial\lambda/\partial\theta_k$. This requires 4 eigenvalue calculations to determine the eigenvalue and its three derivatives. Furthermore, the finite-difference determination of the derivatives involves the finite-difference errors $O(h)$.

The standard approach to following the ray trajectories is to first compute the eigenvalue on a three-dimensional eigenvalue grid. The eigenvalue and its derivatives at any point can then be obtained by interpolation, and the ray trajectories can then be quickly determined using the standard o.d.e. integration. Using the derivative information, the accuracy of the grid interpolation can be substantially improved.

Consider the one-dimensional interpolation case, with a two-point interpolation procedure. Between adjacent points, using only the eigenvalue information, only a linear interpolation is possible. This is second-order accurate in the eigenvalue, and first-order accurate for the derivative. Using derivative information, a cubic interpolation is possible, and this is fourth-order accurate for the eigenvalue and third-
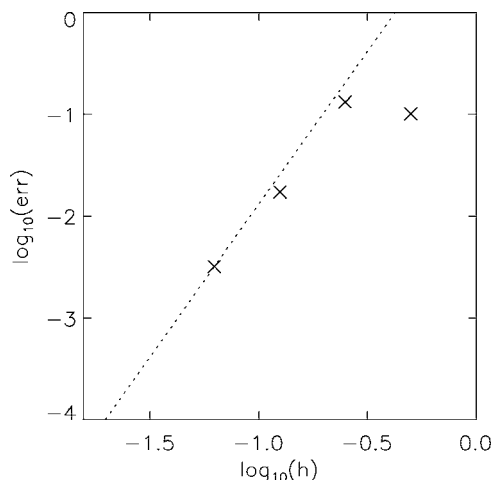
FIG. 1. Scaling of the eigenvalue derivative interpolation error (crosses) with grid spacing h for the example LHD configuration; the third order accuracy (indicated by the dashed line) is confirmed.

order accurate for the derivative. Higher order interpolation schemes are made possible by using additional data points, but always the accuracy of the interpolation can be improved by using the derivative information.

In three dimensions, a tricubic interpolation scheme[11] with C^1 continuity, has been implemented

$$\lambda = \sum_{i=0}^{3} \sum_{j=0}^{3} \sum_{k=0}^{3} a_{i,j,k} x^i y^j z^k, \tag{36}$$

where x, y, z are local interpolation variables, e.g., $x = (\psi - \psi_0)/(\psi_1 - \psi_0)$ where ψ_0, ψ_1 are the adjacent bounding ψ values. The parameters $a_{i,j,k}$ are chosen to match the eigenvalue and its derivatives at each corner of each grid cell. This interpolation gives fourth order accuracy in the grid spacing for the eigenvalue, and third order accuracy for the eigen-
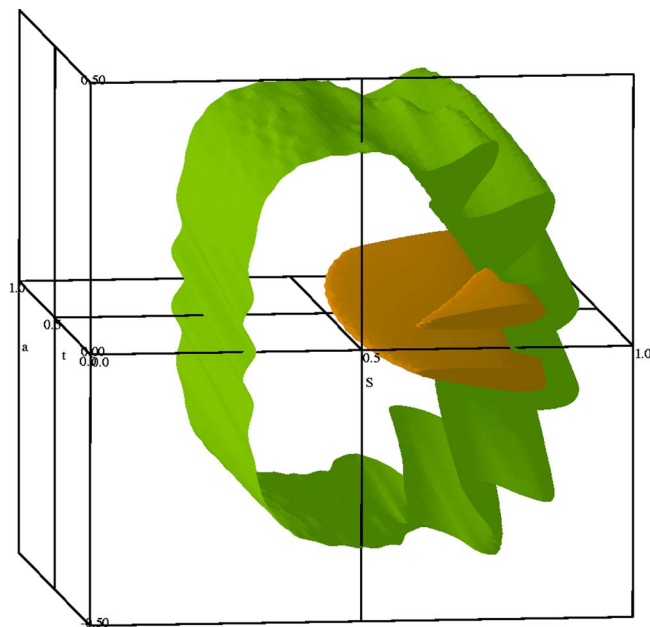

FIG. 2. (Color online) Eigenvalue isosurfaces for the example LHD configuration, showing topologically cylindrical and spherical isosurfaces.

value derivatives. This error scaling has been confirmed, as shown in Fig. 1, for the example LHD configuration. For a given grid resolution, the interpolation error is calculated as the three-dimensional sum of the discrepancy between the interpolated eigenvalue at grid cell midpoint, and the exact eigenvalue. Some example eigenvalue isosurfaces are shown in Fig. 2 for this case. As can be seen, the structure of the eigenvalue in the (ψ, α, θ_k) space is quite detailed, and thus this configuration provides a challenging test of the interpolation procedure. Even for quite crude grid resolutions, with only 2^4 grid points in each dimension, the interpolation errors for the eigenvalue derivative are about 10^{-3}.

Higher order interpolation schemes are also possible in three dimensions, and again the use of the derivatives allows the accuracy of the interpolation to be increased. This significantly reduces the computational burden by allowing accurate interpolation based on relatively coarse eigenvalue grids.

V. DISCUSSION

The use of operator perturbation theory is a computationally efficient approach to determining the eigenvalue derivatives with respect to the ballooning coordinates (ψ, α, θ_k). In the context of the ray tracing problem, it allows the ray trajectories to be determined directly, without the initial step of calculating the eigenvalue on a three-dimensional grid of sufficient resolution to provide the accurate, and smooth, derivatives required for the o.d.e. integration.

In some ray tracing contexts, it may still be convenient to first calculate the eigenvalues on a three-dimensional grid. In this case, the use of the derivatives allows a higher-order interpolation procedure to be implemented.

It not required to use Boozer coordinates for ballooning stability calculations, though from an analytic viewpoint the use of Boozer coordinates does simplify the analysis. For numerical calculations it is computationally efficient to use so-called VMEC coordinates.[10] It is possible to extend the operator perturbation theory to arbitrary coordinate systems.

This method of calculating the derivatives has been numerically implemented and shown to agree with a finite-difference calculation of the derivatives. Application of this approach to ray tracing and the semiclassical quantization of ballooning modes in three-dimensional systems is ongoing.

The example equilibrium has been studied in some detail by Nakajima *et al.*[12] using the global stability code CAS3D. One goal of this research is to compare the results of the ray tracing approach for determining global stability to the global stability results from a global code. This is not a simple task in stellarator geometry. The lack of axisymmetry, in general, results in chaotic ray trajectories and can lead to singular global eigenfunctions. An area of current research is the regularization of this problem by the inclusion of kinetic effects, in particular finite Larmor radius effects. A recent paper by McMillan and Dewar[13] use semiclassical techniques to analyze this effect, and propose a technique to determine the marginal stability boundary even when the rays are chaotic. The quantization of chaotic semiclassical

rays, including the FLR effects, for a LHD relevant equilibrium is beyond the scope of the present article and is left to future work.

[1]R. L. Dewar and A. H. Glasser, Phys. Fluids **26**, 3038 (1983).
[2]W. A. Cooper, D. B. Singleton, and R. L. Dewar, Phys. Plasmas **3**, 275 (1996).
[3]P. Cuthbert, J. L. V. Lewandowski, H. J. Gardner, R. L. Dewar, N. Nakajima, and W. A. Cooper *et al.*, Phys. Plasmas **5**, 2921 (1998).
[4]S. R. Hudson and C. C. Hegna, Phys. Plasmas **11**, L53 (2004).
[5]S. R. Hudson, C. C. Hegna, and N. Nakajima, Nucl. Fusion **45**, 271 (2005).
[6]A. H. Boozer, Phys. Fluids **24**, 1999 (1981).
[7]C. C. Hegna and N. Nakajima, Phys. Plasmas **5**, 1336 (1998).
[8]S. R. Hudson and C. C. Hegna, Phys. Plasmas **10**, 4716 (2003).
[9]R. Sanchez, S. P. Hirshman, J. C. Whitson, and A. S. Ware, J. Comput. Phys. **161**, 576 (2000).
[10]R. Sanchez, S. P. Hirshman, and H. V. Wong, Comput. Phys. Commun. **135**, 82 (2001).
[11]F. Lekien and J. Marsden, Int. J. Numer. Methods Eng. **63**, 455 (2005).
[12]N. Nakajima, S. R. Hudson, and C. C. Hegna, Nucl. Fusion **46**, 177 (2006).
[13]B. F. McMillan and R. L. Dewar, Nucl. Fusion **46**, 477 (2006).